

# An Observational Test of Quantum Cosmology

Steven Gratton\*, Thomas Hertog<sup>†</sup> and Neil Turok<sup>‡</sup>

*DAMTP, Centre for Mathematical Sciences, Wilberforce Rd, Cambridge, CB3 0WA, U.K.*

(August 25, 2021)

## Abstract

We compute the tensor CMB anisotropy power spectrum for singular and non-singular instantons describing the beginning of an open universe according to the Euclidean no boundary proposal. Singular instantons occur generically, whereas non-singular instantons require more contrived scalar field potentials. For the latter, we consider potentials in which a sharp feature, either negative or positive, is added to a gently sloping potential. In the first case one finds a nearly divergent contribution to the low multipole CMB anisotropy, in conflict with the COBE observations. In the second case the divergence is weaker, but matching the low multipoles forces the added feature to be large and narrow. For singular instantons, there is a better match to the observations, without any such contrivance. The distinction between singular and nonsingular instantons disappears in the limit as the universe becomes flat, but is still observable for densities as high as 0.7 of the critical density.

## I. INTRODUCTION

In the most common approach to inflationary theory one postulates a scalar field with a gently sloping potential, and assumes that for some reason the field was initially displaced from the potential minimum. If the initial displacement is large, the field approaches a slowly rolling state in which the universe inflates. This state is an attractor, and in it the system loses memory of the initial conditions. This scenario, which is certainly the simplest version of inflationary theory, predicts that the universe should be flat to high accuracy today. It also predicts that the initial state of the universe should be totally inaccessible to observations today, since the scales most relevant to defining the initial state were stretched by inflation to scales currently exponentially larger than the Hubble radius. If future measurements confirm the universe is very nearly flat, then, assuming inflation is the explanation, discussions of what came before inflation although interesting will remain strictly academic.

---

\*email: S.T.Gratton@damtp.cam.ac.uk

<sup>†</sup>Aspirant FWO-Vlaanderen; email: T.Hertog@damtp.cam.ac.uk

<sup>‡</sup>email: N.G.Turok@damtp.cam.ac.uk

Current CMB observations are consistent with a flat universe, for example the recent Boomerang measurement [1] yields  $0.65 < \Omega_{tot} < 1.45$  at 95 per cent confidence. This lends support to the hope that the simplest version of inflation, described above, might be correct. However, significant space curvature is not yet excluded by the observations. This paper is devoted to examining the observational consequences of inflationary scenarios in which significant space curvature would exist today, and in which the initial conditions for the open universe are actually visible in the microwave sky. In an open universe, the curvature scale of the universe on the surface of last scattering subtends an angular scale of approximately  $\sqrt{\Omega_0}$  radians, about 25 degrees for  $\Omega_0 = 0.3$ . If we live in such a universe, cosmic microwave sky observations can probe the initial conditions for the inflating universe.

Theories of open inflation were initially constructed from scalar field potentials with false vacua, using instantons known as Coleman-De Luccia instantons [5]. These can be interpreted as describing tunnelling from a prior false vacuum inflationary state [6,7], although the relevant instantons only exist for rather special potentials. More recently, however, it was realised that open inflation can occur far more generically through a class of singular, but finite action, instantons [8] which exist for essentially all gently sloping inflationary potentials. The regular instantons do have the virtue that the prediction of  $\Omega$  is unique in a given theory. For the Hawking-Turok instantons, the most probable universe *a priori* is one with a very low value of  $\Omega$ , but there are solutions for essentially all values of  $\Omega$  up to unity. In the absence of a better understanding of how the actual value is determined, which may involve some sort of anthropic considerations, we shall here simply treat the value of  $\Omega$  as a parameter to be adjusted to fit the universe we see. The pattern of density perturbations is then, for given  $\Omega$  and given scalar potential, uniquely predicted.

In this paper we exhibit an interesting observable difference between non-singular and singular instantons. We discuss a generic problem faced by non-singular instantons and show how it is alleviated in singular instantons.

## II. GRAVITATIONAL INSTANTONS AND OPEN INFLATION

Instantons are saddle point solutions of the Euclidean path integral, and open inflationary instantons may be naturally interpreted within the framework of Euclidean quantum gravity and the no boundary proposal [2]. The instantons provide a saddle point, which one can expand around to compute the Euclidean path integral. Correlators of interest are uniquely defined in the Euclidean region, and then analytically continued into the Lorentzian universe. We have recently carried this program through to leading (quadratic) order for scalar and tensor perturbations [3,4]. (Related calculations were performed in a different approach in refs. [11,12].) The well known problems of the non-positivity of the Euclidean Einstein action and the non-renormalisability of quantum gravity do not enter in these low order calculations.

Until recently the class of known cosmological instantons was quite limited. Coleman and De Luccia discovered the first examples when generalising the problem of the decay of a false vacuum in scalar field theory to include gravity [6]. In the limit of weak gravity the decay is well understood and occurs via bubble nucleation. In a localised region of space the scalar field quantum tunnels through the barrier stabilising the false vacuum. The bubble so formed expands at the speed of light and inside it the scalar field rolls down to the true

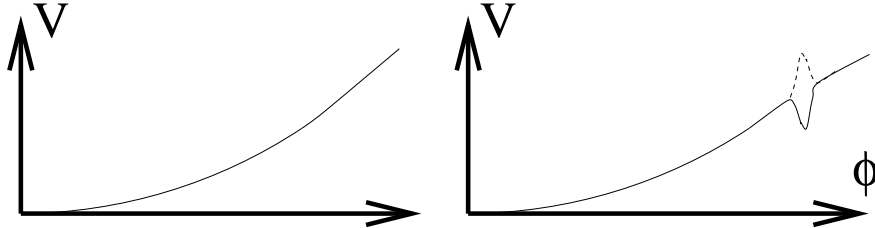


FIG. 1. Inflationary potentials of the types being considered here. The left is a smooth function, like  $m^2\phi^2$ ,  $\lambda\phi^4$  or  $e^{\epsilon\phi}$ . In this theory only Hawking-Turok singular instantons exist. On the right are two potentials allowing Coleman-De Luccia instantons. The solid line shows a potential with a sharp false minimum added, the dashed line one with a sharp maximum.

vacuum. In the presence of gravity, instantons only exist for scalar field potentials with a sufficiently sharp false vacuum (as shown in Figure 1). The reason is that the gravitational instanton has finite size,  $\sim M_{\text{Pl}}/\sqrt{V}$  where  $M_{\text{Pl}}$  is the Planck mass and  $V$  the potential energy density. For an instanton to exist, in which the scalar field is not constant, the scale of variation of the field must be smaller than the instanton size. But this scale of variation is determined by the second derivative of the potential in the region of the barrier,  $|V_{,\phi\phi}| \equiv M^2$ . The condition for existence of Coleman-De Luccia instantons is therefore that  $M^2 \gg V/M_{\text{Pl}}^2$ .

Coleman-De Luccia instantons may be used to describe the nucleation of bubbles in a false vacuum region of de Sitter space [6,7]. The interior of such bubbles then form infinite open universes and with modest fine tuning of the distance  $\Delta\phi$  over which the field rolls during inflation, one can adjust the value of  $\Omega_{\text{tot}}$  to an interesting value less than unity today. But in order for the Coleman-De Luccia instanton to exist, the condition mentioned above must be satisfied. Assume for example that the potential is approximated by  $\frac{1}{2}m^2\phi^2$  in the neighbourhood of the true vacuum, where  $m \ll M_{\text{Pl}}$ . For  $N$  e-folds of inflationary expansion, one requires  $\phi$  to roll for  $2\sqrt{N}M_{\text{Pl}}$  where  $M_{\text{Pl}}$  is the reduced Planck mass. The false vacuum has to be at least this far from the true vacuum. But existence of the Coleman-De Luccia solution requires  $M^2 \gg 4Nm^2$ , and for reasonable  $N > 40$  (for acceptable  $\Omega$  today), the scale  $M$  must be at least an order of magnitude larger than  $m$ . As we show later, yet another tuning is required in order to suppress the large angle CMB anisotropies.

In open inflation, it was assumed that the scalar field became stuck in the false vacuum, leading to large amounts of inflation, in the course of which the universe approached perfect de Sitter space. Bubbles would nucleate in this de Sitter space, as the field tunneled through the barrier between the false and true vacuum states. Each bubble contains an infinite, inflating open universe [6,5].

Coleman-De Luccia instantons have a different interpretation in the no boundary proposal. There they are viewed as classical solutions describing the rounding off of the Lorentzian universe on a compact Euclidean region. The Euclidean path integral uniquely specifies the spectrum of fluctuations inside the bubble without the need for additional assumptions regarding the pre-bubble era. Indeed all calculations that have been performed to date have in effect used the instanton background to define the pre-bubble era. This makes the calculations identical to those performed in the no boundary interpretation. To that extent one can say that all predictions of open inflation are really predictions of the no boundary proposal. The pre-bubble inflating universe appears to be a redundant theoretical

construction.

The Coleman–De Luccia instantons are interesting because they provide a calculable scenario for open inflation. As mentioned the potentials needed to obtain such instantons are necessarily contrived (Figure 1). However Hawking and one of us recently showed that a class of singular but finite action Euclidean instantons exists for almost every gently sloping inflationary potential [8]. We have computed the spectrum of fluctuations about such singular instantons and found that in spite of the singularity the correlators are uniquely defined, just as in the Coleman–De Luccia case [3,4]. Interesting differences arise because the singularity imposes Dirichlet boundary conditions on the perturbation modes. We pointed out that the observational effect of this difference is likely to be most pronounced in the tensor spectrum and this is what we discuss here. We shall show that the part of parameter space for Coleman–De Luccia theories in which the bubble size is much smaller than the De Sitter radius, so that the tunnelling is very similar to that in flat spacetime, is ruled out.

### III. FLUCTUATIONS ABOUT SINGULAR AND NON-SINGULAR INSTANTONS

As we shall see, Coleman–De Luccia instantons with potentials as shown in Figure 1 generically produce a very large amplitude of long wavelength tensor modes. Let us make clear at the outset however that this constraint cannot be used to rule out all such models. The tensor perturbations are governed by the height of the inflationary potential, and can be adjusted independently of the scalar perturbations by flattening the potential. For example potentials of the form used in hybrid inflation, with a flat plateau followed by a sharp drop produce acceptable scalar perturbations but almost no tensor component. Another way of suppressing the low multipoles is to further tune the potential so that it is steep around the values of  $\phi$  where the bubble nucleates [9]. In the light of our discussion above, this constitutes a third fine tuning, needed to make such models work.

In this paper we compare the predictions of singular and Coleman-De Luccia instantons with potentials of the form shown in Figure 1. In the singular case we assume a simple monomial potential like  $\phi^2$  or  $\phi^4$ , and in the Coleman-De Luccia case we superpose a sharp negative false vacuum. We show that unless  $\Omega_{tot}$  is rather close to unity today the Coleman-De Luccia examples are generally ruled out because they predict unacceptable large angle anisotropies in the microwave sky. In contrast the singular instantons which occur generically in gently sloping inflationary potentials appear more compatible with the observations.

In previous work we have derived the two-point correlators of the scalar [3] and tensor [4] metric perturbations in open inflationary universes associated with both classes of Euclidean cosmological instantons. All perturbations are determined from correlators of the gauge-invariant Newtonian potential  $\Psi_N$  and the transverse traceless tensor perturbation  $t_{ij}$ , which may be computed directly from the path integral.

To first order in  $\hbar$  the Euclidean correlators are specified by a Gaussian integral [3,4]. For both regular Coleman–De Luccia instantons and singular instantons the result is unique. In the latter case the singularity enforces Dirichlet boundary conditions. The Euclidean two-point correlators are analytically continued into the Lorentzian region where they describe the quantum mechanical vacuum fluctuations of the various fields in the state described by the no boundary proposal initial conditions.

In the present work we shall calculate the temperature fluctuations on the microwave sky from the Lorentzian two-point correlators. The key observable difference between the two types of instantons occurs for wavelengths of order the curvature scale. Since the long-wavelength continuum in the scalar power spectrum vanishes linearly with wavenumber  $p$ , the differences are small there. Likewise the bound state of the scalar perturbation potential, producing long range correlations beyond the curvature scale in the open universe, is known to have a very minor effect on the CMB anisotropy [10]. However the spectrum of primordial gravity waves has for the regular instantons a near divergence at small  $p$  and therefore provides a better opportunity for a distinguishing test.

The result for the symmetrised two-point correlator tensor metric perturbation about either Hawking–Turok or Coleman–De Luccia instantons is [4]

$$\langle \{t_{ij}(x), t_{i'j'}(x')\} \rangle = 2\kappa\Re \int_0^\infty \frac{dp}{p} \left( \coth p\pi g_p(\tau)g_{-p}(\tau') + r_p \frac{g_p(\tau)g_p(\tau')}{\sinh p\pi} \right) \frac{W_{ij'j'}^{L(p)}(\chi)}{a(\tau)a(\tau')} \quad (1)$$

where  $\kappa = 8\pi G$ , and length units are chosen so that the spatial curvature scale is unity. In this formula  $\tau$  is the conformal time as defined in [3] and  $\chi$  the comoving radial coordinate. The bitensor  $W_{ij'j'}^{L(p)}(\chi)$  is the sum of normalised rank-two tensor harmonics with eigenvalue  $\lambda_p = -(p^2 + 3)$  of the Laplacian on  $H^3$  [4]. The eigenmodes  $g_p(\tau)$  are solutions of the *Lorentzian* tensor perturbation equation

$$\left( -\frac{d^2}{d\tau^2} + \frac{a''}{a} - 1 \right) g_p(\tau) = p^2 g_p(\tau) \quad (2)$$

normalised to obey  $g_p(\tau) \rightarrow e^{-ip\tau}$  as  $\tau \rightarrow -\infty$ .

First note the potential  $p^{-2}$  divergence in the integrand due to the  $1/(p\sinh p\pi)$  in the first term. This divergence, as we shall now argue, is cancelled by the second term. The second term involves  $r_p$  which is a reflection amplitude computed in the Euclidean region. In conformal coordinates the metric takes the form  $b^2(X)(dX^2 + d\Omega_3^2)$ . For singular instantons we have  $0 < X < \infty$  where the singularity is located at  $X = 0$ . For regular instantons we have  $-\infty < X < \infty$ . In both cases the perturbations obey a Schrödinger-like equation with potential  $U(X) \equiv \frac{b''(X)}{b} - 1$ . This potential diverges to  $+\infty$  at  $X = 0$  in the singular case, but is finite everywhere in the regular case. In fact in the latter case it is close to a reflectionless potential  $-2 \operatorname{sech}^2 X$ . The quantity  $r_p$  is in both cases the reflection amplitude for waves incident from  $X = +\infty$ . For singular instantons it is by unitarity a phase but for non-singular instantons it is a complex number of modulus less than unity, and it is small at high  $p$ . Both reflection amplitudes tend to minus one as  $p \rightarrow 0$  because long-wavelength modes are completely reflected, hereby yielding an infrared finite correlator. However, since the non-singular Coleman–De Luccia instantons are much closer to the perfect  $S^4$  non-reflecting solution, we expect the reflection amplitude to tend to  $-1$  at much lower  $p$  than in the singular Hawking–Turok case.

The region of low  $p$  in the the tensor spectrum is what is known in the literature as the bubble wall fluctuation spectrum [10]. When the de Sitter symmetry is only weakly broken, with a scalar field present, there is a near divergence in this spectrum. These long-wavelength tensor perturbations give a substantial contribution to the CMB anisotropies. From the discussion above, we expect a larger contribution to the large angle microwave

anisotropies for regular instantons. In other words, the mild breaking of de Sitter invariance in non-singular models allows for large long-wavelength fluctuations about the background solution. On the contrary, in singular models the deviation from an  $O(5)$  instanton is drastic, and the singularity keeps such fluctuations small.

#### IV. NON-SINGULAR “THIN-WALL” INSTANTONS

The scalar field equation in the Euclidean region reads

$$(b^3\phi_{,\sigma})_{,\sigma} = b^3V_{,\phi}, \quad (3)$$

where  $\sigma$  is the proper radial distance ( $d\sigma = b dX$ ). Following [5] we consider the case where the potential is given by superimposing a sharp negative “bump” of amplitude  $-\Delta V$  centred about  $\phi_f$  onto a smooth monotonically increasing function of  $\phi$ . On a non-singular instanton, the scalar field rolls in the upside down potential from  $\phi_0$ , gaining kinetic energy until it hits the “bump” and rapidly decelerates to an almost standstill near  $\phi_f$ . Effectively all of the kinetic energy of the field is converted to potential energy and any damping is negligible. The field then remains approximately constant as the scale factor  $b$  turns round and vanishes as  $(\sigma_m - \sigma)$ .  $\phi_0$  is fixed by the form of the potential and the requirement of regularity. This generally implies that the scalar field must have reached the “bump” well before the scale factor turns round. We therefore take  $b \approx \sigma$  in equation (3), and approximating  $V_{,\phi}$  as  $V_{,\phi_0} \equiv V_{,\phi}(\phi_0)$ , we have

$$(\sigma^3\phi_{,\sigma})_{,\sigma} \approx \sigma^3V_{,\phi_0}. \quad (4)$$

We have  $\phi_{,\sigma} = 0$  at the regular pole, so we may solve to find

$$\phi \approx \phi_0 + \frac{1}{8} V_{,\phi_0} \sigma^2. \quad (5)$$

If the field approaches the “bump” at  $\sigma_b$ , then its kinetic energy just before hitting the “bump” is

$$\frac{1}{2}\phi_{,\sigma}^2 \approx \frac{1}{32}V_{,\phi_0}^2\sigma_b^2 \approx \frac{1}{4}V_{,\phi_0}(\phi_f - \phi_0) \quad (6)$$

and we may equate this to  $\Delta V$ .

As we shall discuss shortly, it is useful to rewrite the Schrödinger equation in the Euclidean region in a form where it involves the potential  $\bar{U} = \frac{\kappa}{2}\phi'^2$  where prime denotes derivative with respect to conformal coordinate  $X$ . The strength of the potential is then

$$C \equiv \int \frac{\kappa}{2}\phi'^2 dX = \int \frac{\kappa}{2}b\phi_{,\sigma}^2 d\sigma \approx \frac{\kappa}{2} \frac{V_{,\phi_0}^2 \sigma_b^4}{64}. \quad (7)$$

If we take the smooth part of the potential to be of the form  $\lambda\phi^n$ , we may introduce the quantities  $N \equiv \frac{\kappa\phi_0^2}{2n}$  and  $H^2 \equiv \frac{\kappa}{3}V(\phi_0)$ .  $N$  is the slow roll approximation to the number of inflationary efoldings in the open universe.  $H$  is the slow roll Hubble parameter, with  $b \approx \frac{1}{H} \sin H\sigma$ . Then we can write

$$C = \frac{9n(H\sigma_b)^4}{256N}. \quad (8)$$

We will see below that for regular instantons the quantity  $C$  provides an infrared cutoff for the amplitude of the bubble wall fluctuations. From the condition that the scalar field must have reached the bump well before the scale factor turns round, using  $b \approx \frac{1}{H} \sin H\sigma$  we see that  $H\sigma_b$  must certainly be less than  $\frac{\pi}{2}$ . As a concrete example, if we take  $n = 2$  and  $N = 50$ , this yields  $C < 0.01$ . Generically, in the regime where the bubble radius is much smaller than the radius of the de Sitter space,  $C$  will be very much smaller than this, since the formula involves the fourth power of the size of the bubble,  $\sigma_b$ .

## V. NON-SINGULAR “THICK-WALL” INSTANTONS

We now consider instantons associated with potentials with a sharp *positive* feature as shown by the dashed curve in Figure 1. In this case, the scalar field motion is confined within the region of the feature over the instanton, and does not probe the smooth part of the potential at all. Unlike the thin-wall case discussed above, the scalar field varies significantly over the whole instanton, and not just over a localised region of it. The starting value of the scalar field is tuned so that the field reaches the peak of the feature at approximately the same time as the scale factor rolls over. If indeed the potential is exactly symmetrical about the peak over the region probed by the instanton, these two events occur at exactly the same moment. The change in sign of the slope of the potential may then be able to balance the antidamping, bringing the scalar field to a halt as the scale factor again tends to zero, giving us a non-singular solution. For this to occur, the feature must be sufficiently sharp. This can be achieved using differentiable functions with large curvature at the peak. We can model this by introducing a kink. We model the potential in the vicinity of the feature at say  $\phi_*$  as  $V - V_{,\phi} |\phi - \phi_*|$ , with  $V$  and  $V_{,\phi}$  constant and positive. Then we approximate  $b$  as  $1/H \sin H\sigma$ , with  $H^2 = \frac{\kappa}{3}V$ , assuming that  $V$  dominates over gradient energy in the field. In this approximation  $\phi$  reaches  $\phi_*$  at  $\sigma = \pi/2H$ , and  $\phi_{,\sigma}$  is odd about  $\sigma = \pi/2H$ . So in order to calculate  $C = \int \frac{\kappa}{2} b \phi_{,\sigma}^2 d\sigma$ , we need only work out  $\phi_{,\sigma}$  up to  $\sigma = \pi/2H$  and multiply by two. From the scalar field equation we have

$$\begin{aligned} \phi_{,\sigma} &= \frac{V_{,\phi}}{\sin^3 H\sigma} \int_0^\sigma \sin^3 H\sigma d\sigma \\ &= \frac{V_{,\phi} (\cos^3 H\sigma - 3 \cos H\sigma + 2)}{3H \sin^3 H\sigma} \end{aligned} \quad (9)$$

and so

$$\begin{aligned} C &= 2 \times \frac{\kappa}{2} \frac{V_{,\phi}^2}{9H^2} \int_0^{\pi/2H} \frac{1}{H \sin^5 H\sigma} (\cos^3 H\sigma - 3 \cos H\sigma + 2)^2 d\sigma \\ &= \frac{5}{4\kappa} \left( \frac{V_{,\phi}}{V} \right)^2. \end{aligned} \quad (10)$$

We can also integrate Eq. (9) to find that  $\Delta\phi \equiv \phi_* - \phi(0) = 1/2(1 + 2 \ln 2)V_{,\phi}/(\kappa V) \approx 1.19V_{,\phi}/(\kappa V)$ . Inserting into (10) we see that  $C$  can be expressed two ways, either as  $C \approx \Delta\phi V_{,\phi}/V \equiv \Delta V/V$ , or as  $C \approx 0.8\Delta\phi^2/M_{Pl}^2$ , where  $M_{Pl}^2 \equiv \kappa^{-1}$ . We have checked that

the above expressions match the numerically calculated values quite closely up to  $C \sim 1$ . In order to get a value of  $C$  close to unity, one requires a large feature in the potential - i.e. a large change in  $V$  to occur over a range of  $\phi$  which is at least of order unity in (reduced) Planck units. The calculations shown below exclude small values of  $C$ , corresponding in the thick wall case to small positive features on the potential.

## VI. EUCLIDEAN REFLECTION AMPLITUDES AND MODES

The primordial gravity wave spectrum is given by equation (1). In terms of the proper distance  $\sigma$  we used in the previous section, we shall fix the integration constant involved in defining the conformal coordinate  $X$  by setting  $X = \int_{\sigma}^{\sigma_t} \frac{d\sigma'}{b(\sigma')}$ . For non-singular instantons we follow references [3] and [4] and define  $\sigma_t$  to be that value of  $\sigma$  for which  $b$  is maximum. For singular instantons it is taken instead to be the value of  $\sigma$  at the singularity.

For singular instantons, the singularity acts to impose Dirichlet boundary conditions in the Euclidean region. The only allowed mode function at fixed  $p$  is given by  $\psi_p \rightarrow a_p e^{ipX} + a_{-p} e^{-ipX}$  as  $X \rightarrow \infty$ . In the non-singular case, we have left and right moving modes. The left mover is  $g_p^{\text{left}}(X) \rightarrow e^{-ipX}$ , as  $X \rightarrow -\infty$  and  $g_p^{\text{left}}(X) \rightarrow c_p e^{ipX} + d_p e^{-ipX}$  as  $X \rightarrow +\infty$ . These mode functions satisfy the differential equation

$$\left( -\frac{d^2}{dX^2} + U(X) \right) g_p(X) = p^2 g_p(X). \quad (11)$$

which has a trivial bound state solution  $b(X)$  with  $p^2 = -1$ . This corresponds to a constant shift in the metric perturbation which is pure gauge. It is very convenient to project this out, since its presence means that there is an extra phase shift of  $\pi$  produced by the potential even at very low  $p$ . The projection is simple. Rather than  $g$  one considers  $\bar{g} \equiv b\left(\frac{g}{b}\right)'$  which is clearly zero for the bound state [11]. This variable also satisfies a Schrödinger equation

$$\left( -\frac{d^2}{dX^2} + \bar{U}(X) \right) \bar{g}_p(X) = p^2 \bar{g}_p(X) \quad (12)$$

where  $\bar{U}$  is the positive-definite quantity  $\frac{\kappa}{2}\phi'^2$  mentioned in the previous section. We define  $\bar{g}_p(X)$  in an identical fashion. From the constancy of the Wronskian and using  $b \sim e^{-|X|}$  at the regular poles, one finds  $r_p = \frac{1-ip}{1+ip} \bar{r}_p$ . For singular instantons the reflection amplitude  $r_p$  is given by the phase  $\frac{ap}{a-p}$ , and in the non-singular case it equals  $\frac{cp}{d_p}$ . It is straightforward to calculate  $\bar{r}_p$  numerically for any background instanton of interest.

For the non-singular instantons considered in the previous sections  $\bar{U}(X)$  is sharply peaked around a value of  $X$ ,  $X_b$  say. We can then make a very good analytic approximation to  $\frac{\bar{c}_p}{d_p}$  as follows. We replace  $\bar{U}(X)$  by the delta function potential  $C\delta(X - X_b)$  of equivalent strength, with  $C$  as defined in Eq. (7) or Eq. ((10)) as required. We can then solve analytically for  $\bar{g}_p^{\text{left}}(X)$  and find

$$\frac{\bar{c}_p}{d_p} = -\frac{\left(1 + \frac{2ip}{C}\right) e^{-2ipX_b}}{1 + \frac{4p^2}{C^2}}. \quad (13)$$



We approximate  $X_b$  as follows. In the “thin-wall” case  $X_b$  corresponds to  $\sigma = \sigma_b$ . Then with  $b \approx \frac{1}{H} \sin H\sigma$ ,

$$X_b \approx \int_{\sigma_b}^{\sigma_t} \frac{H}{\sin H\sigma} d\sigma \approx -\ln \tan \frac{H\sigma_b}{2} \quad (14)$$

where we have used  $H\sigma_t \approx \frac{\pi}{2}$ . In the “thick-wall” case  $\bar{U}(X)$  is simply peaked around  $\sigma_t$  and so  $X_b \approx 0$ .

## VII. TENSOR CMB ANISOTROPY IN OPEN INFLATION

The Euclidean no boundary path integral allows us to compute correlation functions of any observable. If these correlations are well approximated by a classical statistical distribution, as macroscopic observables such as the microwave anisotropies are, we can regard the predictions as being characterised by the classical distribution. Our observed universe is one member of this classical ensemble. To compare different theories with regard to an observation carried out in our universe, we compute how likely the given observation is according to each theory.

We consider the microwave background anisotropy generated by primordial fluctuations, expanded in spherical harmonics  $\delta T/T = \sum a_{lm} Y_{lm}(\theta, \phi)$ . The  $a_{lm}$ ’s obey  $a_{lm}^* = a_{l-m}$  and we have  $2l + 1$  real observable quantities for each  $l$ . Rotational invariance implies that the  $2l + 1$  quantities are independently distributed with zero mean and common variance  $C_l^{\text{th}}$ . Neglecting higher-order effects, their probability distributions are Gaussian. For a given  $l$  we average over the squares of the  $2l + 1$  observable quantities in our universe to determine  $C_l^{\text{obs}}$ . Then for a given theory of this type,  $C_l^{\text{obs}}/C_l^{\text{th}}$  is  $\chi^2$ -distributed over the ensemble of universes with  $2l + 1$  degrees of freedom.  $C_l^{\text{obs}}$  itself is gamma-distributed with probability density function  $f\left(C_l^{\text{obs}}; \left(l + \frac{1}{2}\right)/C_l^{\text{th}}, l + \frac{1}{2}\right)$  [14]. If  $C_l^{\text{obs}}$  is greater than the median value of  $C_l^{\text{th}}$ , then the fraction of universes with  $C_l$  less likely than  $C_l^{\text{obs}}$  is given by  $2\Gamma\left(l + \frac{1}{2}, \left(l + \frac{1}{2}\right) C_l^{\text{obs}}/C_l^{\text{th}}\right)/\Gamma\left(l + \frac{1}{2}\right)$ . Similarly, if  $C_l^{\text{obs}}$  is less than the median value of  $C_l^{\text{th}}$ , then the fraction of universes with  $C_l$  less likely than  $C_l^{\text{obs}}$  is given by  $2 - 2\Gamma\left(l + \frac{1}{2}, \left(l + \frac{1}{2}\right) C_l^{\text{obs}}/C_l^{\text{th}}\right)/\Gamma\left(l + \frac{1}{2}\right)$ .

We need to obtain the  $C_l^{\text{th}}$ ’s for the different theories we are interested in. Using the usual Sachs-Wolfe formula [15] this is given in terms of our symmetrised tensor correlator (1) as

$$C_l^{\text{th}} = \kappa \Re \int_0^{+\infty} \frac{dp}{2p} \int_{\tau_{\text{ISS}}}^{\tau_{\text{now}}} d\tau \int_{\tau_{\text{ISS}}}^{\tau_{\text{now}}} d\tau' \left( \coth p\pi \left[ \dot{\Phi}_p^L(\tau) \dot{\Phi}_{-p}^L(\tau') \right] + \frac{1}{\sinh p\pi} \left[ r_p \dot{\Phi}_p^L(\tau) \dot{\Phi}_p^L(\tau') \right] \right) Q_{\chi\chi}^{pl} Q_{\chi'\chi'}^{pl}. \quad (15)$$

The primordial tensor power spectrum at the end of inflation defines initial conditions for the Sachs–Wolfe integral. To compute the multipole moments we use CMBFAST [16], which evolves the mode functions from the surface of last scattering at  $\tau_{\text{ISS}}$  up to the present time  $\tau_{\text{now}}$ , given the initial power spectrum. Modifications were required to improve the resolution at low wavenumbers, necessary for the accurate evaluation of the the low  $l$  multipoles.

We then combine the tensor component in the correct ratio [17] with the standard scale invariant scalar spectrum of perturbations in order to obtain the total  $C_l^{\text{th}}$  to compare with experiment. To extract the primordial tensor power spectrum from equation (1), we first construct approximate solutions for the eigenmodes  $g_p^L(\tau) = \Phi_p^L(\tau)a(\tau)$ . In the inflationary phase of the open universe the mode functions closely follow perfect de Sitter evolution in which they tend to a constant after the physical wavelength has been stretched outside the Hubble radius. Hence, to determine the amplitude and phase of this constant we approximate  $a(t)$  as  $\frac{1}{H} \sinh Ht$  until  $\Omega$  is close to one, and introduce the associated conformal coordinate

$$\eta \equiv - \int_t^\infty \frac{H}{\sinh Ht} dt = \ln \tanh \frac{Ht}{2}, \quad (16)$$

$\eta \rightarrow -\infty$  being the start of inflation, and  $\eta \rightarrow 0$  as the universe continues formally to inflate without end.  $\tau - \eta$  is a finite constant during inflation whilst this approximation for  $a(t)$  is a good one. The approximate Lorentzian tensor perturbation equation is then

$$\left( -\frac{d^2}{d\eta^2} + \frac{2}{\cosh^2 \eta} \right) f_p^L(\eta) = p^2 f_p^L(\eta) \quad (17)$$

and the solution in which  $f_p^L(\eta) \rightarrow e^{-ip\eta}$  as  $\eta \rightarrow -\infty$  is

$$f_p^L(\eta) = \frac{ip + \coth \eta}{ip - 1} e^{-ip\eta}. \quad (18)$$

At a given value of  $t$  then, with corresponding  $\tau$  and  $\eta$ , we have  $g_p^L(\tau) \approx e^{-ip(\tau-\eta)} f_p^L(\eta)$ . So dividing by  $a$  and taking the late-time limit we see that

$$\Phi_p(\tau_0) \approx -H \frac{e^{-ip\tau_0}}{ip - 1}. \quad (19)$$

Here  $\tau_0$  is the conformal time as defined in [3] at the end of inflation. This can be calculated numerically and is  $O(1)$  for singular instantons and  $O(0.01)$  for ‘‘thin-wall’’ non-singular instantons. From equation (1) the primordial tensor power spectrum  $P_{\text{T}}(p)$  at the end of inflation is

$$2\kappa\Re \frac{1}{p} \left( \coth p\pi \Phi_p(\tau_0) \Phi_{-p}(\tau_0) + \frac{1 - ip}{1 + ip} \bar{r}_p \frac{\Phi_p(\tau_0) \Phi_p(\tau_0)}{\sinh p\pi} \right). \quad (20)$$

For singular instantons  $\bar{r}_p = \bar{a}_p / \bar{a}_{-p}$  is a phase factor and can be written as  $e^{2i\bar{\theta}_p}$ . So the tensor power spectrum  $P_{\text{T}}^{\text{S}}(p)$  for singular instantons is

$$P_{\text{T}}^{\text{S}}(p) = \frac{2\kappa H^2}{p(1+p^2)} \left( \tanh \frac{p\pi}{2} + \frac{1}{\sinh p\pi} \left( 1 + \frac{1}{1+p^2} \cos 2(\bar{\theta}_p - p\tau_0) \right) \right) \quad (21)$$

in this approximation. For a given potential one evaluates  $\bar{\theta}_p$  numerically and obtains an empirical fit. In the long-wavelength limit  $\bar{\theta}_p \rightarrow -\pi/2$  so the power spectrum is infrared finite. Actually, it turns out that the CMB power spectrum predicted by singular instantons

differs only a little from the one with a perfect reflecting potential in which the ratio  $a_p/a_{-p}$  is replaced by  $-1$  for all  $p$ .

For non-singular instantons, we have  $\bar{r}_p = \bar{c}_p/\bar{d}_p$  in (20). Using our approximations for this in the previous section, we obtain

$$P_{\text{T}}^{\text{NS}}(p) = \frac{2\kappa H^2}{p(1+p^2)} \left( \tanh \frac{p\pi}{2} + \frac{1}{\sinh p\pi} \left( 1 - \frac{\cos 2p(X_b + \tau_0) + \frac{2p}{C} \sin 2p(X_b + \tau_0)}{1 + \frac{4p^2}{C^2}} \right) \right). \quad (22)$$

Equations (21) and (22) define the initial conditions for the numerical computation of the Sachs–Wolfe integral for the different models. A Taylor expansion of the second term around  $p = 0$  shows that in the “thin-wall” case, as speculated earlier [4], for typical values of  $C$  the regime  $c_p/d_p \rightarrow -1$  sets in at much lower  $p$  than in the singular Hawking–Turok case. One can see from (15) that this leads to a larger contribution to the large angle microwave anisotropies for regular “thin-wall” instantons. In the next section we discuss to what extent this characteristic feature of false vacua models allows one to observationally distinguish them from singular open inflation models.

## VIII. NUMERICAL RESULTS

In Figure 2 we compare the CMB anisotropy power spectra for singular and nonsingular instantons, in open universes with  $\Omega_{\text{tot}} = 0.3$  and  $0.7$  respectively. For the nonsingular instantons there is a large contribution from the tensor component, shown by the dashed line. The amplitude of the large angle contribution is governed by the parameter  $C$  discussed above. We argued above that on general grounds  $C$  has to be smaller than  $0.01$  for ‘thin-wall’ instantons. For ‘thick-wall’ instantons  $C$  can be larger if the feature on the potential is large. For singular instantons there is no such parameter to vary. We have chosen  $C = 0.025$  for the nonsingular instantons which is certainly conservative for the thin wall case. The divergence at low  $l$  would be even more pronounced in the allowed regime.

These calculations show that even if the curvature of the universe today is quite modest, one nevertheless sets strong constraints on the form of the inflationary potential and on the nature of the primordial instanton. As emphasised above,  $C$  decreases as the fourth power of the size of the bubble wall thickness - if the latter is much smaller than the Hubble radius of the de Sitter space,  $C$  is much smaller than  $0.01$ . Since the amplitude of the correlator diverges as  $\int dp p^{-2}$ , the amplitude of the quadrupole diverges roughly as  $C^{-1}$ .

In the panels shown the result for the gravity wave spectrum explained above has been combined with the usual scalar spectrum of perturbations appropriate for an open universe [5]. The ratio of tensor to scalar contributions is a function of cosmological and model parameters. However, for medium multipoles, ( $l \sim 30$ ), the ratio approaches its well known flat space value [17]. This value then fixes the relative normalisation of scalar versus tensor anisotropy for all multipoles. For a  $\lambda\phi^n$  inflaton potential the flat space ratio  $R_{\text{fl}} = 0.05n$ . Therefore, the higher the value of  $n$  is, the more important the contribution from the bubble wall tensor fluctuations. In the plots shown we have taken the ratio to be that for  $n = 2$ .

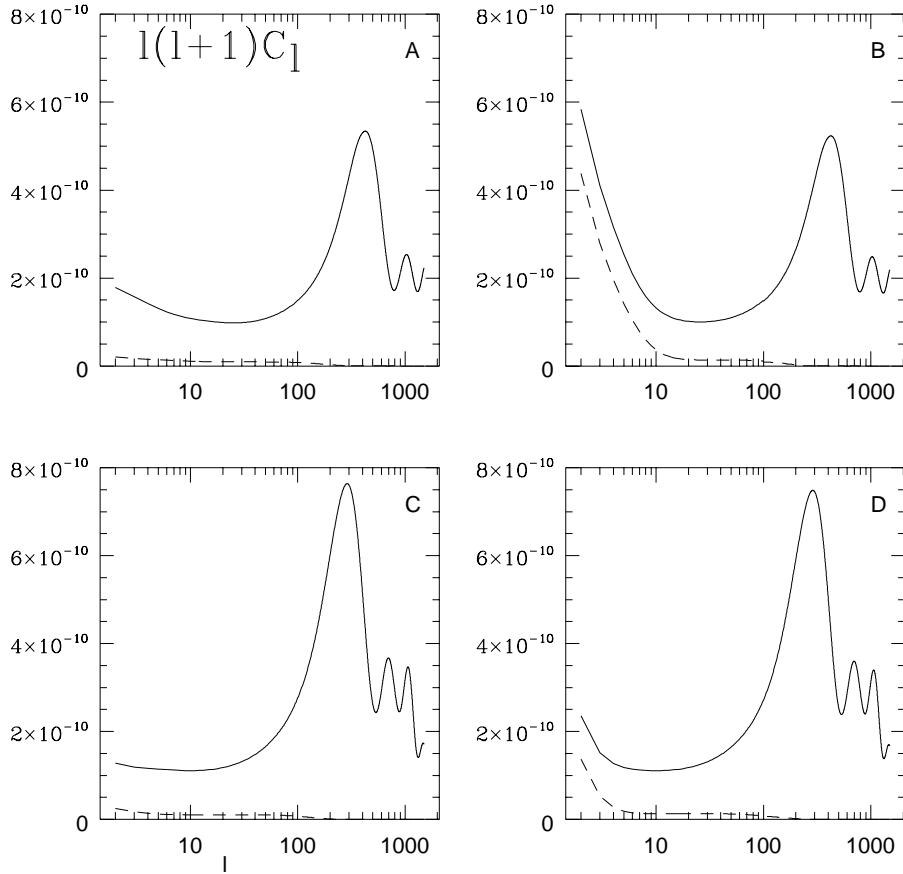


FIG. 2. Cosmic microwave sky predictions of different cosmological instantons. The upper two panels show predictions for an open universe, with  $\Omega_{tot} = 0.3$  and no cosmological constant, for Hawking–Turok (panel A) and Coleman–De Luccia instantons (panel B). The former is for an  $\frac{1}{2}m^2\phi^2$ -potential, the latter for a model where a false vacuum has been added (see text). The lower panels compare the Hawking–Turok (C) and Coleman–De Luccia (D) theories for an  $\Omega_{matter} = 0.3$ ,  $\Omega_{Lambda} = 0.4$ ,  $\Omega_{tot} = 0.7$  cosmology. The difference at low  $l$  is still marked. These results are for a cold dark matter dominated universe with  $\Omega_{CDM} = 0.25$ , baryon density  $\Omega_B = 0.05$ , and Hubble constant  $h = 0.65$ .

This yields a quadrupole ratio  $R_2 \approx 0.13$  in a singular model and  $R_2 \approx 0.57$  in a regular model. Higher values for  $n$  would allow us to exclude the nonsingular models more strongly.

For both singular and non-singular instantons we see the rise in  $C_l^{\text{th}}$  at low  $l$ , characteristic of an open universe. We compare these different models to the COBE DMR data as follows. First of all have to set the overall normalization of each model. We do this with the RADPACK software [18,19]. Using the DMR data alone, we find the normalization which maximizes the likelihood for each model. We then compare likelihoods amongst the different models. The relative likelihoods are as follows:

$$\begin{array}{cccccc} \text{Singular} : & \text{Singular with } \Lambda : & \text{Non-singular} : & \text{Non-singular with } \Lambda : & \text{Flat spectrum} \\ 28 & : & 76 & : & 1 & : & 22 & : & 97 \end{array}$$

where the flat spectrum is one with constant  $l(l+1)C_l$ 's, shown for comparison. In this, Bayesian, approach, the nonsingular instantons for an open universe with  $\Omega_{\text{tot}} = 0.3$  are strongly disfavoured.

Having done the likelihood analysis above, we now take an hypothesis-testing approach, using the probabilities given in Section VII above. The strongest constraint on the models comes from the quadrupole, and we focus on that here. Unfortunately the true sky quadrupole is not yet known, and the literature contains various estimates of it. We have therefore assumed a range of values taken from various references. It is to be hoped that the MAP experiment will accurately determine the actual value.

The model dependence of the low  $l$   $C_l$ 's suggests that in order to quantify the difference between the models we should compare the correctly-normalized predicted quadrupole moments with the measured quadrupole moment. In the table below we show the percentage of universes in the ensemble associated with a given theory with a measured quadrupole more extreme than that seen. We compare the results from singular and non-singular instantons with the best fit flat spectrum for comparison. We have done this for a selection of groups' estimates for the observed quadrupole [20–22]. We have converted all measured values to the dimensionless quantity  $l(l+1)C_l/2\pi$ , dividing by  $(2.73\text{ K})^2$  where necessary, to match the output of CMBFAST. The result from [20] is effectively a direct measurement of the quadrupole, albeit with a systematic error due to the galactic cut. The other results are harder to interpret, having been obtained using maximum likelihood techniques with highly non-Gaussian likelihood functions for the quadrupole [21]. This means that the quoted values below should have large skewed error bars. We also show what a measurement of a larger quadrupole (that from the best fit flat spectrum) would tell us for illustration.

Measured value	Singular $\Omega_\Lambda = 0$	Singular $\Omega_\Lambda = 0.4$	Non-singular $\Omega_\Lambda = 0$	Non-singular $\Omega_\Lambda = 0.4$	Flat spectrum
$3C_2/\pi$	$1.7 \times 10^{-10}$	$1.2 \times 10^{-10}$	$4.0 \times 10^{-10}$	$2.3 \times 10^{-10}$	$1.0 \times 10^{-10}$ [21]
$0.11 \times 10^{-10}$ [20]	0.56%	1.2%	0.071%	0.27%	1.9%
$0.20 \times 10^{-10}$ [21]	2.3%	4.9%	0.31%	1.1%	7.0%
$0.37 \times 10^{-10}$ [22]	9.0%	18%	1.3%	4.6%	25%
$1.0 \times 10^{-10}$ [21]	61%	96%	13%	37%	83%

We note that in general the probability is several times larger for the singular case as compared to the non-singular case. Both models are easier to rule out at a given

confidence level than the flat spectrum. Note that even this model is ruled out at the 98% level if the result of [20] is taken at face value! It should be remembered that for our non-singular “thin-wall” model, we have assumed a value of  $C$  even larger than the extreme best-case. In situations where the theoretical quadrupole is much larger than the measured one, the probability scales as  $(C_2^{\text{meas}}/C_2^{\text{th}}) \sim C^{5/2}$  for the non-singular models. The “thin-wall” nonsingular instantons appear to be strongly ruled out by the observed quadrupole, even if  $\Omega_{tot}$  is as large as 0.7.

## IX. CONCLUSION

We have computed the tensor CMB anisotropy power spectrum for a class of singular and non-singular instantons. We showed that this provides a way to observationally distinguish different versions of open inflation. The “thin-wall” false vacuum models generate larger fluctuations on large angular scales, distinguishing them from singular models. Using the COBE data, we have found that this characteristic feature strongly disfavours “thin-wall” Coleman–De Luccia instantons relative to the singular Hawking–Turok models. Non-singular “thick-wall” Coleman–De Luccia instantons are still viable, but only if the false vacuum feature in the scalar potential is large. In this case the predictions depend strongly on the detailed parameters describing the feature and the models are hence somewhat unattractive. These calculations have therefore enabled us to further constrain the form of the inflaton potential in open inflation.

### Acknowledgements

This work was supported by a PPARC (UK) rolling grant, an EPSRC studentship and a PPARC studentship. We thank L. Knox for providing the RADPACK software used for the likelihood analysis above. We thank M. Bucher, J. Garriga, X. Montes, V. Rubakov, M. Sasaki, T. Tanaka and other participants in the Isaac Newton Institute programme *Structure Formation in the Universe* for very helpful discussions.

## REFERENCES

- [1] A. Melchiorri *et al.*, astro-ph/9911445.
- [2] J.B. Hartle and S.W. Hawking, Phys. Rev. **D28**, 2960 (1983).
- [3] S. Gratton and N. Turok, astro-ph/9902265, Phys. Rev. **D60**, 123507 (1999).
- [4] T. Hertog and N. Turok, astro-ph/9903075 submitted to Phys. Rev. **D**.  
For earlier work on the tensor power spectrum see also  
M. Bucher, J. D. Cohn, Phys. Rev. **D55**, 7461 (97),  
M. Sasaki, T. Tanaka, Progr. Theor. Phys. 97, 243 (97).
- [5] M. Bucher, A.S. Goldhaber and N. Turok, Phys. Rev. **D52**, 3314 (1995).
- [6] S. Coleman and F. De Luccia, Phys. Rev. **D21**, 3305 (1980).
- [7] V.A. Rubakov and S.M. Sibiryakov, gr-qc 9905093.
- [8] S.W. Hawking and N. Turok, Phys. Lett. **B425**, 25 (1998).
- [9] A. Linde, M. Sasaki, T. Tanaka, astro-ph/9901135 (1999).
- [10] J. Garcia-Bellido, hep-ph/9803270.
- [11] J. Garriga, X. Montes, M. Sasaki and T. Tanaka, astro-ph/9811257 (1998).
- [12] J. Garriga, X. Montes, M. Sasaki and T. Tanaka, Nucl. Phys **B513**, 343 (1998).
- [13] J. Garriga, Phys. Rev. **D54**, 4764 (1996),  
J. Garcia-Bellido, Phys. Rev. **D54**, 2473 (1996), astro-ph/9510029; Phys. Rev. **D56**  
(1997) 3225, astro-ph/9702211,  
M. Sasaki, T. Tanaka and Y. Yakushige, Phys. Rev. **D56**, 616 (1997).
- [14] Review of Particle Physics, Phys. Rev. **D54** (1996), p. 157.
- [15] R.K. Sachs and A.M. Wolfe, Astrophys. J. **147**, 73 (1967).
- [16] Available at <http://www.sns.ias.edu/~matiasz/CMBFAST/cmbfast.html>.
- [17] A.R. Liddle and D.H. Lyth, Phys. Lett. **B291**, 391 (1992).
- [18] Available at <http://flight.uchicago.edu/knox/radpack.html>.
- [19] J.R. Bond, A.H. Jaffe, L. Knox, astro-ph/9808264 (1998).
- [20] E.F. Bunn and M. White, ApJ, 480, 6 (1997).
- [21] J.R. Bond, A.H. Jaffe, L. Knox, Phys. Rev. **D57**, 2117 (1998).
- [22] A. Kogut, A.J. Banday, C.L. Bennett, K.M. Gorski, G. Hinshaw, G.F. Smoot and E.L. Wright, Astrophys. J. Lett. **464**, L5 (1996).